Hemangiosarcoma Cells Promote Conserved Host-Derived Hematopoietic Expansion

Jong Hyuk Kim[1-7*], Ashley J. Schulte[1-3], Aaron L. Sarver[1,3,8], Mathew G. Angelos[9,10,11,12], Aric M. Frantz[1-3,13], Colleen L. Forster[14], Timothy D. O'Brien[1,3,9,15], Ingrid Cornax[1,3,15,16], M. Gerard O'Sullivan[1,3,15], Nuojin Cheng[17,18], Mitzi Lewellen[1-3], LeAnn Oseth[3], Sunil Kumar[15], Susan Bullman[19,20], Chandra Sekhar Pedamallu[19,21], Sagar M. Goyal[15], Matthew Meyerson[19,21], Troy C. Lund[3,22], Jessica Alfoldi[19], Matthew Breen[23,24], Kerstin Lindblad-Toh[19,25], Erin B. Dickerson[1-3], Dan S. Kaufman[1,3,9,10,26,27], Jaime F. Modiano[1-3,9,26,28,29]

[1]Animal Cancer Care and Research Program, University of Minnesota, St Paul, MN; [2]Department of Veterinary Clinical Sciences, College of Veterinary Medicine, University of Minnesota, St Paul, MN; [3]Masonic Cancer Center, University of Minnesota, Minneapolis, MN; [4]Department of Small Animal Clinical Sciences, College of Veterinary Medicine, University of Florida, Gainesville, FL; [5]University of Florida Health Cancer Center, University of Florida, Gainesville, FL; [6]Intelligent Critical Care Center, University of Florida, Gainesville, FL; [7]Artificial Intelligence Academic Initiative (AI^2) Center, University of Florida, Gainesville, FL; [8]Institute for Health Informatics, University of Minnesota, Minneapolis, MN; [9]Stem Cell Institute, University of Minnesota, Minneapolis, MN; [10]Department of Medicine (Division of Hematology, Oncology, and Transplantation), Medical School, University of Minnesota, Minneapolis, MN; [11]Microbiology, Immunology and Cancer Biology (MICaB) Graduate Program, University of Minnesota, Minneapolis, MN; [12]Department of Medicine, Division of Hematology and Oncology, School of Medicine, University of Pennsylvania, Philadelphia, PA; [13]Capstan Therapeutics, San Diego, CA; [14]The University of Minnesota Biological Materials

24 Procurement Network (BioNet), University of Minnesota, Minneapolis, MN; [15]Department of
25 Veterinary Population Medicine, College of Veterinary Medicine, University of Minnesota, St
26 Paul, MN; [16]Janssen Research and Development, LLC; [17]School of Mathematics, College of
27 Science and Engineering at the University of Minnesota, Minneapolis, MN; [18]Applied
28 Mathematics, University of Colorado Boulder, Boulder, CO; [19]Broad Institute of MIT and
29 Harvard, Cambridge, MA; [20]Human Biology Division, Fred Hutchinson Cancer Research Center,
30 Seattle, WA; [21]Department of Medical Oncology, Dana-Farber Cancer Institute and Harvard
31 Medical School, Boston, MA; [22]Department of Pediatrics, Medical School, University of
32 Minnesota, Minneapolis, MN; [23]Department of Molecular Biomedical Sciences, College of
33 Veterinary Medicine, & Comparative Medicine Institute, North Carolina State University,
34 Raleigh, NC; [24]Cancer Genetics Program, University of North Carolina Lineberger
35 Comprehensive Cancer Center, Raleigh, NC; [25]Science of Life Laboratory, Department of
36 Medical Biochemistry and Microbiology, Uppsala University, Uppsala, Sweden; [26]Center for
37 Immunology, University of Minnesota, Minneapolis, MN; [27]Division of Regenerative Medicine,
38 Department of Medicine, University of California-San Diego, La Jolla, CA; [28]Department of
39 Laboratory Medicine and Pathology, Medical School, University of Minnesota, Minneapolis,
40 MN; [29]Center for Engineering in Medicine, University of Minnesota, Minneapolis, MN
41
42 *Corresponding author: Jong Hyuk Kim, Department of Small Animal Clinical Sciences,
43 College of Veterinary Medicine, University of Florida, Gainesville, FL 32608
44 Tel.:+1 352-294-4412; E-mail: jkim19@ufl.edu
45
46

Abstract

Hemangiosarcoma and angiosarcoma are soft-tissue sarcomas of blood vessel-forming cells in dogs and humans, respectively. These vasoformative sarcomas are aggressive and highly metastatic, with disorganized, irregular blood-filled vascular spaces. Our objective was to define molecular programs which support the niche that enables progression of canine hemangiosarcoma and human angiosarcoma. Dog-in-mouse hemangiosarcoma xenografts recapitulated the vasoformative and highly angiogenic morphology and molecular characteristics of primary tumors. Blood vessels in the tumors were complex and disorganized, and they were lined by both donor and host cells, a trait that was not observed in xenografts from canine osteosarcoma and lymphoma. In some cases, the xenografted hemangiosarcoma cells created exuberant myeloid hyperplasia and gave rise to lymphoproliferative tumors of mouse origin. We did not uncover a definitive transmissible etiology, but our functional analyses indicate that hemangiosarcoma cells generate a microenvironment that supports expansion and differentiation of hematopoietic progenitor populations. We conclude that canine hemangiosarcomas, and possibly human angiosarcomas, originate from stromal cells that are part of the bone marrow niche and that these cells may also support the growth of hematopoietic tumors.

Significance: We demonstrate that molecular programs supporting expansion of immune and inflammatory cells in hemangiosarcoma resemble those of bone marrow niche cells, providing insights into the potential roles of these cells - whether physiological or pathological - in creating a permissive environment for the progression of hematopoietic malignancies.

70 **Introduction**

71 Canine hemangiosarcoma, a vasoformative tumor originating from bone marrow (BM)-derived
72 progenitor cells, is a common occurrence in dogs, unlike the rare human angiosarcoma (1-4).
73 Tumors from both species exhibit similar histology and natural history of disorganized, tortuous,
74 and dilated blood vessels with high proliferative activity and metastatic potential (5,6).
75 Molecularly, convergent transcriptional programs involving angiogenesis and inflammation are
76 observed in both canine hemangiosarcoma and human angiosarcoma (7,8). While the tumor
77 microenvironment plays a crucial role in tumor cell survival, disease progression, and metastasis
78 through the niche it creates (9), its contribution to the molecular programs of hemangiosarcoma
79 remains incompletely understood. Recent evidence suggests bidirectional interactions between
80 cancer cells and niche cells, where cancer cells re-educate niche cells and vice versa, particularly
81 in maintaining stemness and self-renewal of cancer stem cells in various tumors (9-11), including
82 hematopoietic tumors (12-14).

83

84 The hematopoietic niche is composed of osteoblasts and various stromal cells including endosteal,
85 endothelial cells, fibroblasts, nestin-positive mesenchymal stromal cells, leptin receptor-positive
86 stromal cells, and CXCL12-abundant reticular (CAR) cells. These cells support hematopoiesis by
87 regulating the proliferation and differentiation of hematopoietic stem and progenitor cells (HSPCs)
88 into lineage-committed cells (15). Dysregulation of HSPC function can result in blood disorders
89 (16,17) and hematopoietic malignancies such as leukemia and lymphoma (18-20).

90

91 In the present study, we aimed to elucidate the cellular and molecular origin of canine
92 hemangiosarcoma. Our findings indicate that canine hemangiosarcoma cells not only have the

93 capability to form vasoformative tumors but also create a niche for expansion and differentiation
94 of blood cells, supporting an ontogenetic derivation from bone marrow stromal cells.
95
96 **Results**
97 **Canine hemangiosarcoma cells can recapitulate the disease *in vivo***
98 We used *in vivo* xenografts to investigate the biological behavior of canine hemangiosarcoma (21-
99 25). Mice were inoculated with canine hemangiosarcoma cell lines or primary tissues, as detailed
100 in **Supplementary Table S1**. However, the engraftment efficiency of canine hemangiosarcoma
101 xenografts was found to be low. Only cultured DHSA-1426 cells, when injected subcutaneously,
102 consistently generated vasoformative tumors in immunodeficient beige-nude-xid (BNX) mice
103 (**Figure 1**). The tumorigenic potential of this cell line was maintained over multiple passages, as
104 demonstrated by serial passaging of cells cultured from tumor xenografts into new recipient mice
105 (**Supplementary Figure S1**).
106
107 **Xenografts allow quantification of the stromal contribution in the hemangiosarcoma**
108 **microenvironment**
109 To establish the contribution of stromal elements to the formation of canine hemangiosarcoma, we
110 utilized fluorescence *in situ* hybridization (FISH) to quantify the presence of both canine and
111 mouse cells in the tumors. Specifically, we employed probes for canine *CXCL8*, as this gene is
112 absent in the mouse genome, and a unique region of the mouse X chromosome, to differentiate
113 between canine and mouse cells, respectively. Our data revealed that the hemangiosarcoma
114 xenografts displayed a complex topological organization, with blood vessels lined by both donor
115 and host cells (**Figure 2A**). Notably, the organization pattern observed in canine hemangiosarcoma

116 xenografts differed from that of canine osteosarcoma and lymphoma xenografts (**Figure 2B**). The
117 hemangiosarcoma tumors were comprised of a mixture of 50-70% malignant canine cells and 30-
118 50% mouse stromal cells. The cellular composition of orthotopic osteosarcoma xenografts was
119 comparable, but without malignant canine cells lining blood vessels. In contrast, lymphoma
120 xenografts exhibited a markedly distinct composition, with less than 5% mouse stromal cells and
121 the absence of malignant canine cells from blood vessels **(Figure 2C**). These findings highlight
122 the utility of xenografts as a valuable tool for quantifying the contribution of stromal elements to
123 the tumor microenvironment.
124
125 To gain a deeper understanding of the involvement of stromal elements in canine
126 hemangiosarcoma xenografts, we analyzed RNA-seq data obtained from cells and xenografts. The
127 RNA-seq data was mapped to a reference genome that included both canine and mouse cells (26).
128 Notably, we observed that the RNA-seq data from the cell lines predominantly mapped to the
129 canine genome, whereas the xenografts exhibited mapping to both the canine and mouse genomes,
130 which was consistent with the results obtained from FISH (**Supplementary Figure S2;**
131 **Supplementary Table S2**).
132
133 **Canine xenografts generate lymphomas of mouse origin**
134 An unexpected series of findings shed light on the relationship between hemangiosarcoma and
135 inflammation in the microenvironment. Previous studies, including our own, have demonstrated
136 that canine hemangiosarcoma cells can successfully form hemangiosarcomas in NSG mice (21-
137 25). However, we noted instances where NSG mice, following inoculation with SB
138 hemangiosarcoma cells or another cell line named Emma-brain (EFB), and BNX mice, following

139 inoculation with tumor fragments derived from sample DHSA-1426 (freshly obtained from a dog
140 with spontaneous hemangiosarcoma), developed round cell tumors. Notably, four out of five mice
141 that received 5×10^6 SB hemangiosarcoma cells intraperitoneally and one out of four mice that
142 received 2×10^6 EFB cells subcutaneously, succumbed acutely two weeks after inoculation,
143 displaying signs of anemia and splenomegaly. Histological examination revealed that the spleens
144 of these mice were expanded by monomorphic populations of hematopoietic cells (**Figure 3A, B**).
145 Upon further analysis, the cells were determined to be of mouse origin and represented erythroid
146 progenitors (Ter-119+), with a few canine hemangiosarcoma cells admixed in the population
147 (**Figure 3C-F**). However, we were unable to definitively establish whether these cells had
148 undergone malignant transformation.
149
150 Three of four mice that received DHSA-1426 tumor fragments, representing 1st-generation canine
151 patient-derived xenograft (CPDX), developed tumors in multiple organs, including spleen, lymph
152 nodes, meninges, cerebrum, and mesentery, 12 weeks after implantation. However, the
153 morphology of these tumors resembled that of round cell tumors (**Supplementary Figure S3A,**
154 **B**). Immunohistochemical analysis showed that the tumor cells expressed CD45, B220, and Pax5,
155 but did not express CD3, Ter-119, and MPO (**Supplementary Figure S3C-H**), indicating a mouse
156 B-cell origin. To further verify the mouse origin of these cells, flow cytometry was conducted,
157 revealing positive staining for mouse CD45, but not for canine CD45 or human αVβ3-integrin
158 (CD51/CD61), which exhibits cross-reactivity with canine, but not with mouse αVβ3-integrin
159 (**Supplementary Figure S4**). Furthermore, RNA-seq data from the mouse round cell tumors
160 demonstrated a near-complete alignment with the mouse genome, consistent with the findings

161 from flow cytometry (**Supplementary Figure S2**), thereby indicating that the tumors were derived
162 from mouse cells.
163
164 The malignant B-cells demonstrated the ability to undergo serial passage and establish B-cell
165 lymphomas in recipient BNX mice independently, without the requirement for canine
166 hemangiosarcoma cell support (**Supplementary Figure S5**). Intriguingly, similar results were
167 obtained when single cell suspensions derived from fresh tumor fragments of canine
168 hemangiosarcoma xenografts were inoculated into BNX recipients, representing 2nd generation
169 CPDX derived from a 1st generation cell line tumor. The resulting tumors of mouse B-cell origin
170 displayed comparable morphology and were likewise amenable to serial passage in BNX mice.
171
172 The potential etiology of these tumors was perplexing. To investigate the possibility of a
173 transmissible, infectious agent as the cause of these tumors, we sequenced RNA from the
174 xenografts and used the PathSeq platform for analysis. However, no bacterial or viral sequences
175 with tumorigenic potential were identified in the xenografts or in the primary or metastatic canine
176 hemangiosarcoma tumor samples or cell lines. While a recent study reported an association
177 between *Bartonella spp*. and canine hemangiosarcoma (27,28), only 10 of 24 dogs tested in our
178 study had detectable *Bartonella spp*. sequences, and these were present in low abundance
179 (**Supplementary Table S3**). Furthermore, four of the samples contained sequences from *B.*
180 *bacilliformis, B. grahamii*, or *B. tribocorum*, which infect humans and rats, respectively, and are
181 not known to infect dogs as primary or accidental hosts (29,30). Three of the remaining six dogs
182 had sequences for *B. clarridgeiae*, and three had sequences for multiple *Bartonella spp.*, including

183 human and rodent-specific types. The low abundance and the presence of sequences from
184 organisms that do not infect dogs suggest that the *Bartonella spp.* sequences were contaminants.
185
186 In contrast, murine leukemia virus (MuLV) reads were consistently identified in mouse B-cell
187 lymphomas that arose from the hemangiosarcoma xenografts (**Supplementary Table S4**). The
188 presence of MuLV sequences was further confirmed in one mouse B-cell lymphoma arising from
189 hemangiosarcoma xenografts and in two subcutaneous canine hemangiosarcoma xenograft tumors
190 through independent viral RNA sequencing experiments. Additionally, MuLV sequences were
191 detected by polymerase chain reaction (PCR) in normal mouse tissues (liver and spleen), as well
192 as in each of the three mouse B-cell lymphomas arising from the hemangiosarcoma xenografts and
193 two subcutaneous canine hemangiosarcoma xenograft tumors. Notably, MuLV was also found in
194 SB hemangiosarcoma cells that had been previously passaged through mice as hemangiosarcomas,
195 suggesting that MuLV is a promiscuous virus with potential involvement in these tumors. These
196 findings also suggested that MuLV might be the transforming agent responsible for the
197 development of mouse lymphomas, and raised the possibility that canine hemangiosarcoma cells
198 could provide a conducive environment for the expansion of these MuLV-transformed B-cells.
199
200 **Human and canine hemangiosarcoma tissues show evidence of immune cells.**
201 We reanalyzed RNA-Seq data obtained from both canine hemangiosarcoma and human
202 angiosarcoma samples, with the aim of investigating the presence of immune cells within the tumor
203 microenvironment. To identify co-expressed genes without bias, we used an unbiased approach
204 called GCESS (Gene Cluster Expression Summary Score) (31). Notably, the highest expression of
205 these immune signature genes was observed in the inflammatory subtype of canine

206 hemangiosarcoma (**Supplementary Figure S6**). We next segregated human angiosarcomas into
207 tumors with high and low immune scores ("immune-high" vs "immune-low") and identified 461
208 up-regulated genes (FDR $P < 0.05$) in the immune-high group compared to immune-low group
209 (**Figure 4A)**. Fifty-eight of these genes were also found in canine inflammatory
210 hemangiosarcomas, and they were associated with T- and B-cell activation (**Figure 4B, C**). This
211 approach allowed us to identify a common immune signature in both human and canine tumors.
212
213 To confirm whether the inflammatory gene signatures were originating from the malignant cells
214 themselves or from inflammatory cells within the tumors, we employed bioinformatics tools and
215 immunostaining techniques. Tumor purity was assessed using ESTIMATE and immune scores
216 were assigned to each tumor using *xCell*. Both tools yielded consistent scores (**Supplementary**
217 **Figure S7A, B**). As expected, we found a correlation between immune scores and the predominant
218 transcriptional phenotype of the tumor in both canine and human samples (**Supplementary Figure**
219 **S7C-F**). Specifically, angiogenic tumors exhibited low immune scores, whereas inflammatory
220 tumors exhibited high immune scores.
221
222 To further validate that the observed immune signatures were the result of immune and
223 inflammatory cells present within the tumors, we performed immunohistochemical staining on
224 sections from 11 canine hemangiosarcomas and 10 human angiosarcomas. Antibodies against T
225 cells (CD3), B cells (Pax5), myeloid cells (Mac387), and macrophages (Iba1 for canine; CD163
226 for human) were used; CD3+ T cells, Pax5+ B cells, Mac387+ myeloid cells, and Iba1+ or
227 CD163+ macrophages were present in both canine and human tumors (**Figure 4D, E**). Myeloid
228 cells were the most abundant, while T cells varied in frequency from rare to abundant, and B cells

229 were infrequent. Importantly, the distribution of inflammatory cells was diffuse throughout the
230 tumor tissue. Furthermore, there was a direct correlation between xCell immune scores and
231 immunohistochemistry scores for both canine (Spearman R=0.38; P = 0.255) and human
232 (Spearman R=0.78; P = 0.011) samples that were examined (**Figure 4F, G**). These findings
233 provide evidence that the observed immune signatures in both canine and human tumors are likely
234 attributed to the presence of immune and inflammatory cells within the tumor microenvironment.
235

236 **Canine hemangiosarcoma cells promote and maintain hematopoiesis**

237 To determine whether hemangiosarcoma cells were functionally sufficient to expand
238 hematopoietic progenitor cells *in vitro*, we conducted long-term culture initiating cell (LTC-IC)
239 assays using DHSA-1426 and EFB canine hemangiosarcoma cells, to assess their potential in
240 promoting and maintaining hematopoiesis in CD34+ human umbilical cord blood hematopoietic
241 progenitor cells (HPCs). Mouse M2-10B4 and human bone marrow-derived mesenchymal stromal
242 cells (MSCs) were used as positive controls, while HPCs cultured without feeder cells served as a
243 negative control. Remarkably, DHSA-1426 cells were found to promote expansion of human
244 CD34+ HPCs with at least comparable, if not superior, efficiency compared to conventional mouse
245 or human feeder cells, and resulted in comparable proportions of hematopoietic cell differentiation
246 *in vitro* across all lineages (**Figure 5; Supplementary Figure S8**). Similar results were observed
247 with EFB cells, albeit with slightly more limited expansion and differentiation.
248

249 **Discussion**

250 Vasoformative sarcomas are aggressive tumors with uncertain cellular origin, proposed to arise
251 from a multipotent bone marrow cell or lineage-committed endothelial progenitor cells in humans,

252 dogs, and mice (1-4,8). While human angiosarcomas and canine hemangiosarcomas have a limited
253 shared mutational spectrum, primarily in visceral forms of the disease and human breast
254 angiosarcomas, convergent transcriptional programs characterized by deregulation of
255 phosphoinositide 3-kinase pathways are activated in tumors of both species, as well as in zebrafish
256 (8,32-38).
257
258 The transcriptional landscape of human angiosarcoma and canine hemangiosarcoma is strongly
259 pro-angiogenic. However, a subset of tumors in both species exhibit robust transcriptional immune
260 and inflammatory signatures that correlate with the presence of T cells and macrophages. The
261 presence of immune and inflammatory infiltrates might be associated with longer survival
262 outcomes, but further research is needed to determine their clinical significance regarding disease
263 progression and their association with the approximately 15% of exceptional survivors reported in
264 canine hemangiosarcoma (39,40).
265
266 The findings from our xenograft experiments provide further evidence supporting the concept that
267 the disordered vascular organization in these tumors is driven by the tumor cells (1,21,25). Our
268 experiments reveal that the tumor vessels are comprised of both malignant tumor cells and non-
269 malignant host endothelial cells, a phenomenon that appears to be unique to hemangiosarcoma
270 among the three types of xenografts we investigated. This observation underscores the ability of
271 hemangiosarcoma cells to adopt endothelial functions and suggests that non-malignant cells play
272 a role in the formation of aberrant blood vessels in vasculogenic tumors.
273

274 Interestingly, our experiments also demonstrate that the stromal cells in these xenografts contribute
275 to the angiogenic and inflammatory transcriptional signatures. Our preliminary data further
276 suggest that genes expressed by CAR cells, sinusoidal stromal cells, endosteal niche cells,
277 endothelial progenitors, and hematopoietic progenitors (such as CSF3, IL6, IL11, and LIF) are
278 enriched in canine hemangiosarcoma tissues and cells. This highlights the possibility that the
279 stromal cells themselves are also influenced or reprogrammed by the malignant cells and supports
280 a complex interplay between the tumor and its microenvironment. These findings highlight a
281 potential vulnerability in the formation of the hemangiosarcoma niche, where the interactions
282 between the tumor cells and their microenvironment are tightly orchestrated.
283
284 The initial perplexity surrounding the development of exuberant myeloid and erythroid
285 hyperplasia, as well as bona fide lymphomas, arising from mouse cells in animals with primary or
286 secondary hemangiosarcoma xenografts has led us to investigate the underlying etiology. Our
287 results suggest that a transmissible etiology from dog to mouse is unlikely to be the cause of these
288 expanded hematopoietic cell populations. Instead, our data indicate that canine hemangiosarcomas
289 have the capability to support robust expansion and differentiation of hematopoietic progenitor
290 cells *in vitro*, which may account for the expansion of myeloid cells *in vivo* in mice and in primary
291 canine and human tumors. This expansion of non-malignant hematopoietic progenitor cells and
292 mature leukocytes may also explain why clonal mutations (34) and fusions (8) are found less often
293 in the inflammatory subtype of canine hemangiosarcoma.
294
295 In the case of lymphomas that occurred repeatedly and independently in animals receiving
296 different tumor preparations, MuLV might have driven the transformation of residual lymphoid

297 elements within a hyperproliferative environment created by the hemangiosarcoma cells. These
298 findings are consistent with a previous report of angiosarcoma in the bone marrow of a human
299 patient with tumor-associated myeloid proliferation and extramedullary hematopoiesis (41).
300
301 Other unexpected tumors have been reported in xenograft experiments and preclinical models of
302 stem cell transplantation. For example, transplantation of murine MSCs has been shown to induce
303 tumor formation and tissue malformation, possibly due to genetic instability and/or cellular
304 transformation (42-44). Similarly, patient-derived xenografts of human solid cancers, such as
305 breast, colon, pancreatic cancer, and rhabdomyosarcoma, have been reported to induce
306 lymphomagenesis or lymphocytic tumors in immunodeficient mice, but in these cases, the tumors
307 were derived from human tumor-infiltrating lymphocytes transformed by Epstein-Barr virus (45-
308 48). Importantly, these previously reported tumors were all of donor origin, while the tumors
309 observed in our study originated from the mouse recipients and were distinct from the donor
310 hemangiosarcomas.
311
312 We were unable to find any reports of hematopoietic tumors of recipient origin arising from
313 xenotransplantation experiments using other types of canine cancers in the literature, and we have
314 not observed such events in our own studies (26,49,50). Thus, this finding appears to be unique to
315 canine hemangiosarcoma and may be attributed to the ability of hemangiosarcoma cells to support
316 hematopoietic expansion. Our findings also suggest that the normal counterparts of canine
317 hemangiosarcoma cells might contribute to the development of hematopoietic malignancies
318 through the creation of a permissive niche.
319

320 In this context, it is noteworthy that a shared region of the canine genome has been found to be
321 significantly associated with B-cell lymphomas, hemangiosarcomas, and other blood derived
322 tumors in various breeds of dogs belonging to distinct genetic clades (51-53). This finding
323 highlights the intriguing possibility of a molecular connection between these seemingly distinct
324 tumors, suggesting that disruptions in hematopoiesis and cellular reprogramming may contribute
325 to their development (54). It also sets the origin of this potential genomic vulnerability prior to the
326 derivation of modern dog breeds.
327
328 The capacity of the hematopoietic niche to accommodate bone marrow transplants and adoptive
329 cell therapies has revealed its resilience, with bone marrow stromal cells exhibiting high resistance
330 to chemotherapy and radiation. These intrinsic properties may explain the relatively poor long-
331 term responses of human patients with angiosarcoma and dogs with hemangiosarcoma to cytotoxic
332 therapies, and they could provide opportunities for the development of more effective treatments.
333 However, it is important to recognize that therapies targeting the hematopoietic niche may also
334 carry the potential for high toxicity.
335
336 Our data present a novel model to elucidate the etiology and cell of origin of canine
337 hemangiosarcomas, and potentially human angiosarcomas. We propose that the malignant cells
338 originate from bone marrow nurse cells, which have the capability to create niches that promote
339 angiogenic proliferation or hematopoietic expansion, as illustrated in **Figure 6**. The robust
340 inflammation observed in some of these tumors may therefore be intrinsic to the tumor itself, rather
341 than solely due to extrinsic factors associated with tissue disruption. These paths of differentiation

342 may also influence the biological behavior of the tumors, with those exhibiting strong angiogenic
343 propensity displaying more aggressive behaviors (8).
344
345 In conclusion, our study adds to the growing body of evidence demonstrating the complex
346 interactions between tumor cells and the host microenvironment. Importantly, our data do not
347 support a transmissible etiology for hemangiosarcoma. However, they do suggest that the
348 permissive niche created by these cells can lead to the development of hematopoietic tumors driven
349 by leukemia viruses in mice, raising the possibility that the bone marrow niche plays a similar role
350 in viral lymphomas and leukemias in humans. Further investigations are warranted to unravel the
351 underlying mechanisms that drive these observations and ascertain their significance in the
352 development of human cancer.
353

354 **Materials and Methods**

355 **Human tissue samples**

356 The human angiosarcoma tissue samples used in this study were formalin-fixed and paraffin-
357 embedded, as previously described (8). The samples were obtained from two sources: the
358 University of Minnesota Biological Materials Procurement Network and the Cooperative Human
359 Tissue Network. All sample acquisitions were performed under standardized patient consent
360 protocols.
361

362 **Canine tissue samples and cell lines**

363 Previously established hemangiosarcoma cell lines (SB, COSB, Emma, DD1, JHE, and JLU)
364 (1,2,4,21,25,55) were used in this study. Canine tissue samples were collected from surgical

365 removals or tumor biopsies at the University of Minnesota or private veterinary clinics. Additional
366 hemangiosarcoma cell lines (DHSA-1401, DHSA-1420, and DHSA-1426) were generated and
367 cultured using established methods (1,2,55). Cell line authentication for canine cells were
368 conducted by IDEXX BioAnalytics (Columbia, MO, USA). All sample acquisition procedures
369 were approved by the Institutional Animal Care and Use Committee (IACUC) of the University
370 of Minnesota under protocols 0802A27363, 1101A94713, and 1312-31131A.
371
372 **Human and mouse cell lines**
373 Human bone marrow-derived mesenchymal stromal cells (hBM-MSCs) were isolated from whole
374 bone marrow purchased from AllCells (Emeryville, CA, USA), as described previously (56-59).
375 M2-10B4 murine bone marrow stromal cells were purchased from the ATCC (Manassas, VA,
376 USA) and maintained following established protocols (57). Samples of human umbilical cord
377 blood (hUCB) were obtained from the ClinImmune Stem Cell Laboratory at the University of
378 Colorado Cord Blood Bank (60).
379
380 **Mice and xenotransplantation**
381 We conducted multiple xenograft experiments using various cell lines and patient-derived tumor
382 sections. First, we injected cultured-tumor cells from three hemangiosarcoma cell lines (SB,
383 Emma, and JHE) into NSG mice. Specifically, we injected 5×10^6 SB cells subcutaneously in four
384 mice, and 5 or 10×10^6 SB cells intraperitoneally in four mice. Additionally, we injected 2×10^6
385 Emma cells subcutaneously and intraperitoneally in four mice each, and 3×10^5 JHE cells
386 subcutaneously in four mice. Next, we injected tumor cells from five hemangiosarcoma cell lines
387 (Emma, DD1, JLU, DHSA-1401, and COSB) into NSG neonates, 1 or 2 days after birth. We

388 injected 5 × 10^5 Emma, DD1, JLU, or DHSA-1401 cells, or 6.25 × 10^5 COSB cells
389 intraperitoneally in 50 μL of PBS. We also injected 5 × 10^6 cells from three hemangiosarcoma cell
390 lines (JLU, DHSA-1420, and DHSA-1426) in a mixture of 100 μL of PBS and 100 μL of BD
391 Matrigel™ Basement Membrane Matrix into the subcutaneous space of BNX mice. For DHSA-
392 1426, we injected tumor cells from passage-5 and passage-14 independently. We used sections of
393 viable tumors from four dogs affected with hemangiosarcoma and implanted them into
394 subcutaneous pockets of four mice for each dog. In addition, we implanted sections of non-
395 hemangiosarcoma splenic tissues from seven dogs into 18 mice as controls. Finally, after visible
396 tumors developed in mice, we serially transplanted the tumors by inoculation of cultured tumor
397 cells in three mice or by direct implantation of single-cell suspensions of the tumor in eight mice.
398 We monitored the mice for tumor development and sacrificed them when they reached a tumor
399 endpoint, including a mass measuring 1.5 cm in the longest diameter or at the end of a 16-week
400 period after xenotransplantation. All animal procedures were conducted in accordance with the
401 Research Animal Resources (RAR) husbandry and care protocols and reviewed and approved by
402 the IACUC of the University of Minnesota (protocols 1006A84813, 1106A00649, 1306-30712A,
403 and 1311-31104A). A total of 132 mice were used for xenotransplantation procedures, as described
404 in **Supplementary Table S1**.
405
406 **Flow cytometric analysis**
407 We used the following antibodies for flow cytometry analysis of xenograft tumors: rat anti-dog
408 CD45-APC (Clone YKIX716.13; AbD Serotec, Raleigh, NC, USA), rat anti-mouse CD45-APC
409 (Clone 30-F11; eBioscience, San Diego, CA, USA), and mouse anti-human αvβ3 (CD51/CD61)-
410 FITC (Clone 23C6; BD Pharmingen, San Jose, CA, USA). Isotype controls included rat IgG2b-

411 APC (Clone eB149/10H5; eBioscience) and mouse IgG1 K-FITC (Clone P3.6.2.8.1; eBioscience).
412 Data were acquired using a BD Acuri C6 flow cytometer (BD Biosciences, San Jose, CA) and
413 analyzed with FlowJo software (version 10.1, Tree Star, Ashland, OR, USA).
414
415 **Immunohistochemistry**
416 Immunohistochemical staining was conducted at either the BioNet Histology Laboratory,
417 Minnesota Veterinary Diagnostic Laboratory, or Comparative Pathology Shared Resource at the
418 University of Minnesota. The following antibodies were used: CD3, PAX5, MAC387, CD163,
419 CD204, Iba1, Ter-119, MPO, and CD45. Details of the antibodies used are provided in
420 **Supplementary Table S5**.
421
422 **RNA-seq for gene expression profiling**
423 To obtain transcriptomic profiles, we isolated total RNA from xenograft tumor samples using the
424 TriPure Isolation Reagent (Roche Applied Science, Penzberg, Germany), followed by clean-up
425 using the RNeasy Mini Kit (Qiagen). We generated RNA-seq libraries with a targeted depth of 20
426 million paired-end reads (2 x 50 bp) at the UMGC, as previously described (4,8). We conducted
427 bioinformatic analyses for gene expression profiling as previously reported (4,8,26,31,61). RNA-
428 seq data from human angiosarcoma tissues can be accessed via the Gene Expression Omnibus
429 (GEO) under accession number GSE163359 (8). RNA-Seq data from canine hemangiosarcoma
430 tissues are available through the GEO (accession number GSE95183) and the NCBI Sequence
431 Read Archive (accession number PRJNA562916) (8).
432
433 **Viral RNA isolation and library generation**

434 To detect RNA viruses, we isolated viral RNA from xenograft tumors using either a Qiagen viral
435 RNA kit or Trizol followed by the Qiagen viral RNA kit (Qiagen, Germantown, MD, USA). The
436 isolated RNA was then submitted to the University of Minnesota Genomics Center (UMGC) for
437 viral RNA MiSeq. The Illumina MiSeq generated approximately 1 million paired-end reads (2 x
438 250) for each sample.
439
440 **PathSeq analysis**
441 The PathSeq algorithm was used to determine transmissible agents in RNA-seq data from dog and
442 mouse samples. The PathSeq algorithm (62) was used to perform computational subtraction of
443 mouse and dog genomes followed by alignment of residual reads to mouse and dog reference
444 genomes and microbial reference genomes (including bacterial, viral, archaeal, and fungal
445 sequences downloaded from NCBI). These alignments resulted in the identification of microbial
446 reads in the data. Human reads were subtracted by first mapping reads to a database of mouse
447 (mm9) and dog reference genomes (canFam3.1; GCF_000002285) using BWA (Release 0.6.1,
448 default settings) (63), MegaBLAST (Release 2.2.25, cut-off E-value 10^{-7}, word size 16) and
449 BLASTN (Release 2.2.25, cut-off E-value 10^{-7}, word size 7, nucleotide match reward 1, nucleotide
450 mismatch score -3, gap open cost 5, gap extension cost 2) (64). Only sequences with perfect or
451 near perfect matches to the human genome were removed in the subtraction process. In addition,
452 low complexity and highly repetitive reads were removed using RepeatMasker (version open-
453 3.3.0) (65). To identify microbial reads, the residual reads were aligned with MegaBLAST to a
454 database of microbial and dog reference genomes. Raw read counts were calculated using the reads
455 that were mapped to *Epstein-Barr virus* (EBV) and *H. pylori* with at least 90% identity and 90%
456 query coverage. Using the raw read counts, the abundance metric or normalized read count of a

457 given microbe in a sample was calculated as

458 $$Abundance\ metric = \left(\frac{\#\ reads\ mapped\ to\ the\ microbe}{\left(\frac{\#\ reads\ in\ the\ sample}{Average\ \#\ reads\ in\ the\ sample\ cohort} \right) * \left(\frac{Genome\ size\ of\ the\ microbe}{Average\ genome\ size\ of\ the\ microbes\ in\ that\ kingdom} \right)} \right)$$

459 Relative abundance in a given sample was calculated as abundance metric of taxa divided by the
460 total abundance metric at kingdom level of the sample.

461

462 **Long-term culture initiating cell (LTC-IC) and hematopoietic colony forming unit (CFU)**
463 **assays**

464 We isolated human umbilical cord blood (hUCB) CD34+ cells from two patients using the
465 Miltenyi CD34 Microbead Kit and MACS separation column (Miltenyi Biotec, Boston, MA,
466 USA), following the manufacturer's instructions. The purity of isolated hUCB CD34+ cells was
467 determined by flow cytometry using the following antibodies (all anti-human): CD34-PECy7
468 (eBioscience, San Diego, CA, USA), CD43-APC (BD Biosciences, San Jose, CA, USA), and
469 CD45-APC (BD Biosciences). Sorted hUCB CD34+ cells with >92% CD34+CD45+ were used
470 for subsequent experiments. We seeded M2-10B4, hBM-MSCs, 1426, and Emma in gelatin-coated
471 24-well plates at a density of 10^5 cells/well overnight. After inactivation with 10 μg/mL Mitomycin
472 C for three hours, 5,000 hUCB CD34+ cells were added to each well in Myelocult H5100
473 (StemCell Technologies, Vancouver, BC, Canada) supplemented with 1μM dexamethasone
474 (Sigma-Aldrich, St. Louis, MO, USA). Gelatin-coated wells without stroma were used as negative
475 controls. Cells were conditioned for six weeks at 37°C and 5% CO_2 with one-half media exchanges
476 every week. At week 5, non-adherent cells from selected wells were harvested, counted, and
477 analyzed for hematopoietic-specific surface antigens using the following antibodies (all anti-
478 human): CD34-PECy7, CD33-APC (BD Biosciences), CD43-APC and CD45-APC. At the end of

479 the six-week culture, both non-adherent and adherent cells were collected using 0.05% trypsin
480 supplemented with 2% chicken serum for five minutes. Cells were filtered using a 70 μm cell
481 strainer to generate single-cell suspensions and counted. We prepared triplicate CFU assays by
482 seeding 50,000 cells/1.5 mL of semi-solid Methocult H4435 Enriched media (StemCell
483 Technologies) in 35 mm culture dishes (Greiner, Monroe, NC, USA). After two additional weeks,
484 the plates were manually scored for total number and phenotype of the CFUs, as previously
485 described (66).
486
487 **Statistical analysis**
488 Pearson and Spearman correlation coefficient was calculated for correlation between two
489 variables. Statistical analysis was performed using GraphPad Prism 9 (GraphPad Software, Inc.,
490 San Diego, CA, USA) or Microsoft Excel.
491
492 **Data Availability**
493 The data generated in this study are publicly available in GEO at GSE163359 and GSE95183, as
494 well as in NCBI Sequence Read Archive (PRJNA562916). Other relevant data generated in this
495 study are available upon request from the corresponding author.
496
497 **Disclosure of Conflicts of Interest**
498 No potential conflicts of interest were disclosed.
499
500 **Authors' Contributions**
501 Conception and design: J.H. Kim, J.F. Modiano

502 Development of methodology: J.H. Kim, A.L. Sarver, M.G. Angelos, A.M. Frantz, S. Bullman,
503 C.S. Pedamallu, S. Kumar, S.M. Goyal, L. Oseth, C.L. Foster, T.D. O'Brien, I. Cornax, J.F.
504 Modiano
505 Acquisition of data (provided animals, acquired and managed patients, provided facilities, etc):
506 M.G. O'Sullivan, M. Meyerson, T.C. Lund, J. Alfoldi, M. Breen, K. Lindblad-Toh, D.S.
507 Kaufman, J.F. Modiano
508 Analysis and interpretation of data (e.g., statistical analysis, biostatistics, computational
509 analysis): J.H. Kim., A.L. Sarver., M.G. Angelos, A.M. Frantz, N. Cheng., J. Alfoldi., K.
510 Lindblad-Toh, S. Bullman, C.S. Pedamallu
511 Writing, review, and/or revision of the manuscript: J.H. Kim, A.J. Schulte, E.B. Dickerson, D.S.
512 Kaufman, J.F. Modiano
513 Administrative, technical, or material support (i.e., reporting or organizing data, constructing
514 databases): J.H. Kim, A.J. Schulte, M. Lewellen.
515 Study supervision: J.H. Kim, J.F. Modiano
516
517 **Acknowledgements**
518 The authors acknowledge Keumsoon Im for assistance with experiments and data acquisition.
519 The authors would also like to acknowledge Milcah Scott for processing the next generation
520 sequencing data and assistance with data analysis. Artistic design of Figures 2A and 7 was
521 created with Biorender (biorender.com). This work was partially supported by grants
522 1R03CA191713-01 (to J.F. Modiano, A.L. Sarver, and J.H. Kim) from the NCI of the NIH,
523 grants #02759 (to J.H. Kim), #422 (to J.F. Modiano), and 1889-G (to J.F. Modiano, M. Breen,
524 and K. Lindblad-Toh) from the AKC Canine Health Foundation, grant JHK15MN-004 (to J.H.

525 Kim, A.L. Sarver, J.F. Modiano) from the National Canine Cancer Foundation, grant D10-501
526 (to J.F. Modiano, M. Breen, and K. Lindblad-Toh) from Morris Animal Foundation, and grant
527 from Swedish Cancerfonden (to K. Lindblad-Toh). This work was supported by an NIH NCI
528 R50 grant, CA211249 (to A.L. Sarver). It was also supported by a Career Development Award
529 from the Department of Defense Peer Reviewed Cancer Research Program (to J.H.Kim). The
530 NIH Comprehensive Cancer Center Support Grant to the Masonic Cancer Center, University of
531 Minnesota (P30 CA077598) provided support for the cytogenetic analyses performed in the
532 Cytogenomics Shared Resource. M. Breen is supported in part by the Oscar J. Fletcher
533 Distinguished Professorship in Comparative Oncology Genetics at North Carolina State
534 University. K. Lindblad-Toh is supported by a Distinguished Professor award from the Swedish
535 Research Council. J.F. Modiano is supported by the Alvin and June Perlman Chair in Animal
536 Oncology. The authors gratefully acknowledge donations to the Animal Cancer Care and
537 Research Program of the University of Minnesota that helped support this project. The content of
538 this manuscript is solely the responsibility of the authors and does not necessarily represent the
539 official views of any of the funding agencies listed above.
540

541 **References**

542 1. Fosmire SP, Dickerson EB, Scott AM, Bianco SR, Pettengill MJ, Meylemans H*, et al.*
543 Canine malignant hemangiosarcoma as a model of primitive angiogenic endothelium. Lab
544 Invest **2004**;84:562-72
545 2. Lamerato-Kozicki AR, Helm KM, Jubala CM, Cutter GC, Modiano JF. Canine
546 hemangiosarcoma originates from hematopoietic precursors with potential for endothelial
547 differentiation. Exp Hematol **2006**;34:870-8

548 3. Liu L, Kakiuchi-Kiyota S, Arnold LL, Johansson SL, Wert D, Cohen SM. Pathogenesis of
549 human hemangiosarcomas and hemangiomas. Hum Pathol **2013**;44:2302-11
550 4. Gorden BH, Kim JH, Sarver AL, Frantz AM, Breen M, Lindblad-Toh K*, et al.* Identification
551 of three molecular and functional subtypes in canine hemangiosarcoma through gene
552 expression profiling and progenitor cell characterization. Am J Pathol **2014**;184:985-95
553 5. Italiano A, Thomas R, Breen M, Zhang L, Crago AM, Singer S*, et al.* The miR-17-92 cluster
554 and its target THBS1 are differentially expressed in angiosarcomas dependent on MYC
555 amplification. Genes Chromosomes Cancer **2012**;51:569-78
556 6. Kim J-H, Graef A, Dickerson E, Modiano J. Pathobiology of Hemangiosarcoma in Dogs:
557 Research Advances and Future Perspectives. Vet Sci **2015**;2:388
558 7. Tamburini BA, Phang TL, Fosmire SP, Scott MC, Trapp SC, Duckett MM*, et al.* Gene
559 expression profiling identifies inflammation and angiogenesis as distinguishing features of
560 canine hemangiosarcoma. BMC Cancer **2010**;10:619
561 8. Kim JH, Megquier K, Thomas R, Sarver AL, Song JM, Kim YT*, et al.* Genomically
562 Complex Human Angiosarcoma and Canine Hemangiosarcoma Establish Convergent
563 Angiogenic Transcriptional Programs Driven by Novel Gene Fusions. Mol Cancer Res
564 **2021**;19:847-61
565 9. Quail DF, Joyce JA. Microenvironmental regulation of tumor progression and metastasis.
566 Nat Med **2013**;19:1423-37
567 10. Colmone A, Amorim M, Pontier AL, Wang S, Jablonski E, Sipkins DA. Leukemic cells
568 create bone marrow niches that disrupt the behavior of normal hematopoietic progenitor
569 cells. Science **2008**;322:1861-5

570 11. Schreiber RD, Old LJ, Smyth MJ. Cancer immunoediting: integrating immunity's roles in
571 cancer suppression and promotion. Science **2011**;331:1565-70
572 12. Lane SW, Scadden DT, Gilliland DG. The leukemic stem cell niche: current concepts and
573 therapeutic opportunities. Blood **2009**;114:1150-7
574 13. Charles N, Ozawa T, Squatrito M, Bleau AM, Brennan CW, Hambardzumyan D*, et al.*
575 Perivascular nitric oxide activates notch signaling and promotes stem-like character in
576 PDGF-induced glioma cells. Cell Stem Cell **2010**;6:141-52
577 14. Vermeulen L, De Sousa EMF, van der Heijden M, Cameron K, de Jong JH, Borovski T*, et*
578 *al.* Wnt activity defines colon cancer stem cells and is regulated by the microenvironment.
579 Nat Cell Biol **2010**;12:468-76
580 15. Adams GB, Scadden DT. The hematopoietic stem cell in its place. Nat Immunol **2006**;7:333-
581 7
582 16. de Haan G, Lazare SS. Aging of hematopoietic stem cells. Blood **2018**;131:479-87
583 17. Filippi MD, Ghaffari S. Mitochondria in the maintenance of hematopoietic stem cells: new
584 perspectives and opportunities. Blood **2019**;133:1943-52
585 18. Wu JY, Purton LE, Rodda SJ, Chen M, Weinstein LS, McMahon AP*, et al.* Osteoblastic
586 regulation of B lymphopoiesis is mediated by Gs{alpha}-dependent signaling pathways. Proc
587 Natl Acad Sci U S A **2008**;105:16976-81
588 19. Raaijmakers MH, Mukherjee S, Guo S, Zhang S, Kobayashi T, Schoonmaker JA*, et al.* Bone
589 progenitor dysfunction induces myelodysplasia and secondary leukaemia. Nature
590 **2010**;464:852-7
591 20. Kode A, Manavalan JS, Mosialou I, Bhagat G, Rathinam CV, Luo N*, et al.* Leukaemogenesis
592 induced by an activating beta-catenin mutation in osteoblasts. Nature **2014**;506:240-4

593 21. Akhtar N, Padilla ML, Dickerson EB, Steinberg H, Breen M, Auerbach R*, et al.* Interleukin-
594 12 inhibits tumor growth in a novel angiogenesis canine hemangiosarcoma xenograft model.
595 Neoplasia **2004**;6:106-16
596 22. Kodama A, Sakai H, Matsuura S, Murakami M, Murai A, Mori T*, et al.* Establishment of
597 canine hemangiosarcoma xenograft models expressing endothelial growth factors, their
598 receptors, and angiogenesis-associated homeobox genes. BMC Cancer **2009**;9:363
599 23. Murai A, Asa SA, Kodama A, Hirata A, Yanai T, Sakai H. Constitutive phosphorylation of
600 the mTORC2/Akt/4E-BP1 pathway in newly derived canine hemangiosarcoma cell lines.
601 BMC Vet Res **2012**;8:128
602 24. Andersen NJ, Nickoloff BJ, Dykema KJ, Boguslawski EA, Krivochenitser RI, Froman RE*, et*
603 *al.* Pharmacologic inhibition of MEK signaling prevents growth of canine hemangiosarcoma.
604 Mol Cancer Ther **2013**;12:1701-14
605 25. Kim JH, Frantz AM, Anderson KL, Graef AJ, Scott MC, Robinson S*, et al.* Interleukin-8
606 promotes canine hemangiosarcoma growth by regulating the tumor microenvironment. Exp
607 Cell Res **2014**;323:155-64
608 26. Scott MC, Tomiyasu H, Garbe JR, Cornax I, Amaya C, O'Sullivan MG*, et al.* Heterotypic
609 mouse models of canine osteosarcoma recapitulate tumor heterogeneity and biological
610 behavior. Dis Model Mech **2016**;9:1435-44
611 27. Lashnits E, Neupane P, Bradley JM, Richardson T, Thomas R, Linder KE*, et al.* Molecular
612 prevalence of Bartonella, Babesia, and hemotropic Mycoplasma species in dogs with
613 hemangiosarcoma from across the United States. PLoS One **2020**;15:e0227234

614 28. Varanat M, Maggi RG, Linder KE, Breitschwerdt EB. Molecular prevalence of Bartonella,
615 Babesia, and hemotropic Mycoplasma sp. in dogs with splenic disease. J Vet Intern Med
616 **2011**;25:1284-91
617 29. Chomel BB, Boulouis HJ, Maruyama S, Breitschwerdt EB. Bartonella spp. in pets and effect
618 on human health. Emerg Infect Dis **2006**;12:389-94
619 30. Engel P, Dehio C. Genomics of host-restricted pathogens of the genus bartonella. Genome
620 Dyn **2009**;6:158-69
621 31. Scott MC, Temiz NA, Sarver AE, LaRue RS, Rathe SK, Varshney J*, et al.* Comparative
622 Transcriptome Analysis Quantifies Immune Cell Transcript Levels, Metastatic Progression,
623 and Survival in Osteosarcoma. Cancer Res **2018**;78:326-37
624 32. Choorapoikayil S, Weijts B, Kers R, de Bruin A, den Hertog J. Loss of Pten promotes
625 angiogenesis and enhanced vegfaa expression in zebrafish. Dis Model Mech **2013**;6:1159-66
626 33. Wang G, Wu M, Maloneyhuss MA, Wojcik J, Durham AC, Mason NJ*, et al.* Actionable
627 mutations in canine hemangiosarcoma. PLoS One **2017**;12:e0188667
628 34. Megquier K, Turner-Maier J, Swofford R, Kim JH, Sarver AL, Wang C*, et al.* Comparative
629 Genomics Reveals Shared Mutational Landscape in Canine Hemangiosarcoma and Human
630 Angiosarcoma. Mol Cancer Res **2019**;17:2410-21
631 35. Wang G, Wu M, Durham AC, Radaelli E, Mason NJ, Xu X*, et al.* Molecular subtypes in
632 canine hemangiosarcoma reveal similarities with human angiosarcoma. PLoS One
633 **2020**;15:e0229728
634 36. Beca F, Krings G, Chen YY, Hosfield EM, Vohra P, Sibley RK*, et al.* Primary mammary
635 angiosarcomas harbor frequent mutations in KDR and PIK3CA and show evidence of
636 distinct pathogenesis. Mod Pathol **2020**;33:1518-26

637 37. Chan JY, Lim JQ, Yeong J, Ravi V, Guan P, Boot A*, et al.* Multiomic analysis and
638 immunoprofiling reveal distinct subtypes of human angiosarcoma. J Clin Invest
639 **2020**;130:5833-46
640 38. Painter CA, Jain E, Tomson BN, Dunphy M, Stoddard RE, Thomas BS*, et al.* The
641 Angiosarcoma Project: enabling genomic and clinical discoveries in a rare cancer through
642 patient-partnered research. Nat Med **2020**;26:181-7
643 39. Borgatti A, Koopmeiners JS, Sarver AL, Winter AL, Stuebner K, Todhunter D*, et al.* Safe
644 and Effective Sarcoma Therapy through Bispecific Targeting of EGFR and uPAR. Mol
645 Cancer Ther **2017**;16:956-65
646 40. Borgatti A, Fieberg A, Winter AL, Stuebner K, Taras E, Todhunter D*, et al.* Impact of
647 repeated cycles of EGF bispecific angiotoxin (eBAT) administered at a reduced interval from
648 doxorubicin chemotherapy in dogs with splenic haemangiosarcoma. Vet Comp Oncol
649 **2020**;18:664-74
650 41. Xie W, Lin P, Konoplev S. An unexpected diagnosis: angiosarcoma with bone marrow
651 involvement mimicking a myeloproliferative neoplasm. Br J Haematol **2019**;184:495
652 42. Miura M, Miura Y, Padilla-Nash HM, Molinolo AA, Fu B, Patel V*, et al.* Accumulated
653 chromosomal instability in murine bone marrow mesenchymal stem cells leads to malignant
654 transformation. Stem Cells **2006**;24:1095-103
655 43. Foudah D, Redaelli S, Donzelli E, Bentivegna A, Miloso M, Dalpra L*, et al.* Monitoring the
656 genomic stability of in vitro cultured rat bone-marrow-derived mesenchymal stem cells.
657 Chromosome Res **2009**;17:1025-39

658 44. Jeong JO, Han JW, Kim JM, Cho HJ, Park C, Lee N, *et al.* Malignant tumor formation after
659 transplantation of short-term cultured bone marrow mesenchymal stem cells in experimental
660 myocardial infarction and diabetic neuropathy. Circ Res **2011**;108:1340-7
661 45. Chen K, Ahmed S, Adeyi O, Dick JE, Ghanekar A. Human solid tumor xenografts in
662 immunodeficient mice are vulnerable to lymphomagenesis associated with Epstein-Barr
663 virus. PLoS One **2012**;7:e39294
664 46. Fujii E, Kato A, Chen YJ, Matsubara K, Ohnishi Y, Suzuki M. Characterization of EBV-
665 related lymphoproliferative lesions arising in donor lymphocytes of transplanted human
666 tumor tissues in the NOG mouse. Exp Anim **2014**;63:289-96
667 47. Bondarenko G, Ugolkov A, Rohan S, Kulesza P, Dubrovskyi O, Gursel D, *et al.* Patient-
668 Derived Tumor Xenografts Are Susceptible to Formation of Human Lymphocytic Tumors.
669 Neoplasia **2015**;17:735-41
670 48. Tillman H, Vogel P, Rogers T, Akers W, Rehg JE. Spectrum of Posttransplant
671 Lymphoproliferations in NSG Mice and Their Association With EBV Infection After
672 Engraftment of Pediatric Solid Tumors. Vet Pathol **2020**;57:445-56
673 49. Weiskopf K, Anderson KL, Ito D, Schnorr PJ, Tomiyasu H, Ring AM, *et al.* Eradication of
674 Canine Diffuse Large B-Cell Lymphoma in a Murine Xenograft Model with CD47 Blockade
675 and Anti-CD20. Cancer Immunol Res **2016**;4:1072-87
676 50. Ito D, Endicott MM, Jubala CM, Helm KM, Burnett RC, Husbands BD, *et al.* A tumor-
677 related lymphoid progenitor population supports hierarchical tumor organization in canine B-
678 cell lymphoma. J Vet Intern Med **2011**;25:890-6

679 51. Tonomura N, Elvers I, Thomas R, Megquier K, Turner-Maier J, Howald C*, et al.* Genome-
680 wide association study identifies shared risk loci common to two malignancies in golden
681 retrievers. PLoS Genet **2015**;11:e1004922
682 52. Hédan B, Cadieu É, Rimbault M, Vaysse A, Dufaure de Citres C, Devauchelle P*, et al.*
683 Identification of common predisposing loci to hematopoietic cancers in four dog breeds.
684 PLoS Genet **2021**;17:e1009395
685 53. Evans JM, Parker HG, Rutteman GR, Plassais J, Grinwis GCM, Harris AC*, et al.* Multi-
686 omics approach identifies germline regulatory variants associated with hematopoietic
687 malignancies in retriever dog breeds. PLoS Genet **2021**;17:e1009543
688 54. Zhang Q, Orlando EJ, Wang HY, Bogusz AM, Liu X, Lacey SF*, et al.* Transdifferentiation of
689 lymphoma into sarcoma associated with profound reprogramming of the epigenome. Blood
690 **2020**;136:1980-3
691 55. Tamburini BA, Trapp S, Phang TL, Schappa JT, Hunter LE, Modiano JF. Gene expression
692 profiles of sporadic canine hemangiosarcoma are uniquely associated with breed. PLoS One
693 **2009**;4:e5549
694 56. Hicok KC, Thomas T, Gori F, Rickard DJ, Spelsberg TC, Riggs BL. Development and
695 characterization of conditionally immortalized osteoblast precursor cell lines from human
696 bone marrow stroma. J Bone Miner Res **1998**;13:205-17
697 57. Kopher RA, Penchev VR, Islam MS, Hill KL, Khosla S, Kaufman DS. Human embryonic
698 stem cell-derived CD34+ cells function as MSC progenitor cells. Bone **2010**;47:718-28
699 58. Zou L, Kidwai FK, Kopher RA, Motl J, Kellum CA, Westendorf JJ*, et al.* Use of RUNX2
700 expression to identify osteogenic progenitor cells derived from human embryonic stem cells.
701 Stem Cell Reports **2015**;4:190-8

702 59. Zou L, Chen Q, Quanbeck Z, Bechtold JE, Kaufman DS. Angiogenic activity mediates bone
703 repair from human pluripotent stem cell-derived osteogenic cells. Sci Rep **2016**;6:22868
704 60. Ferrell PI, Hexum MK, Kopher RA, Lepley MA, Gussiaas A, Kaufman DS. Functional
705 assessment of hematopoietic niche cells derived from human embryonic stem cells. Stem
706 Cells Dev **2014**;23:1355-63
707 61. Cheng N, Schulte AJ, Santosa F, Kim JH. Machine learning application identifies novel gene
708 signatures from transcriptomic data of spontaneous canine hemangiosarcoma. Brief
709 Bioinform **2021**;22:bbaa252
710 62. Kostic AD, Ojesina AI, Pedamallu CS, Jung J, Verhaak RG, Getz G*, et al.* PathSeq: software
711 to identify or discover microbes by deep sequencing of human tissue. Nat Biotechnol
712 **2011**;29:393-6
713 63. Li H, Durbin R. Fast and accurate short read alignment with Burrows-Wheeler transform.
714 Bioinformatics **2009**;25:1754-60
715 64. Altschul SF, Madden TL, Schäffer AA, Zhang J, Zhang Z, Miller W*, et al.* Gapped BLAST
716 and PSI-BLAST: a new generation of protein database search programs. Nucleic Acids Res
717 **1997**;25:3389-402
718 65. Smit A HR, Green P. **RepeatMasker Open-3.0**. <http://www.repeatmasker.org>.
719 66. Kaufman DS, Hanson ET, Lewis RL, Auerbach R, Thomson JA. Hematopoietic colony-
720 forming cells derived from human embryonic stem cells. Proc Natl Acad Sci U S A
721 **2001**;98:10716-21

Figure 1

A

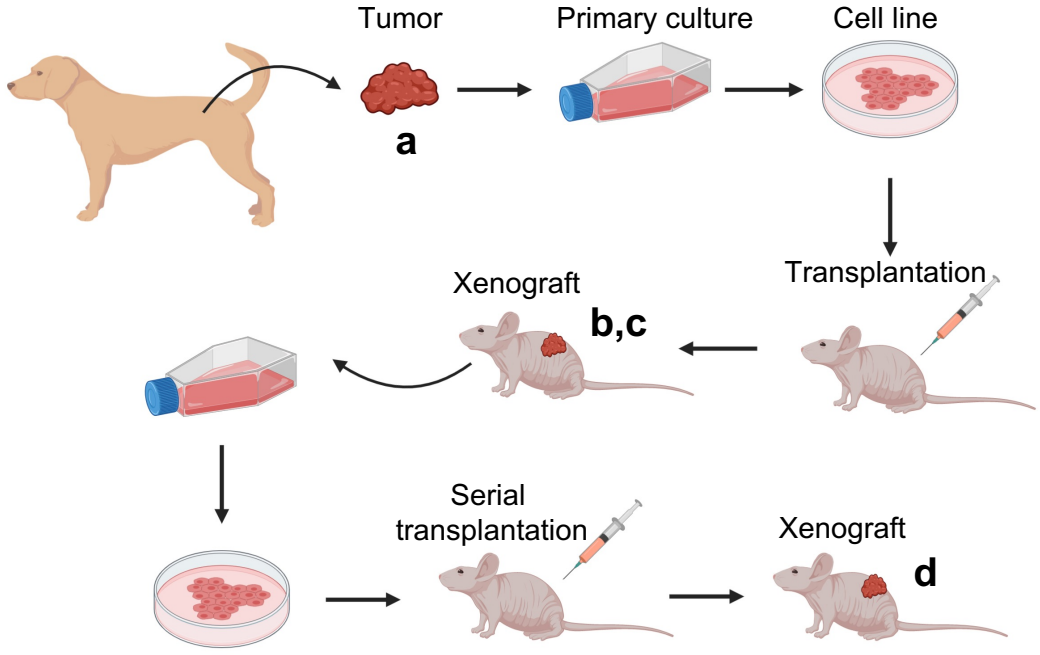
Tumor
Primary culture
Cell line
a
Transplantation
Xenograft
b,c
Serial
transplantation
Xenograft
d

B

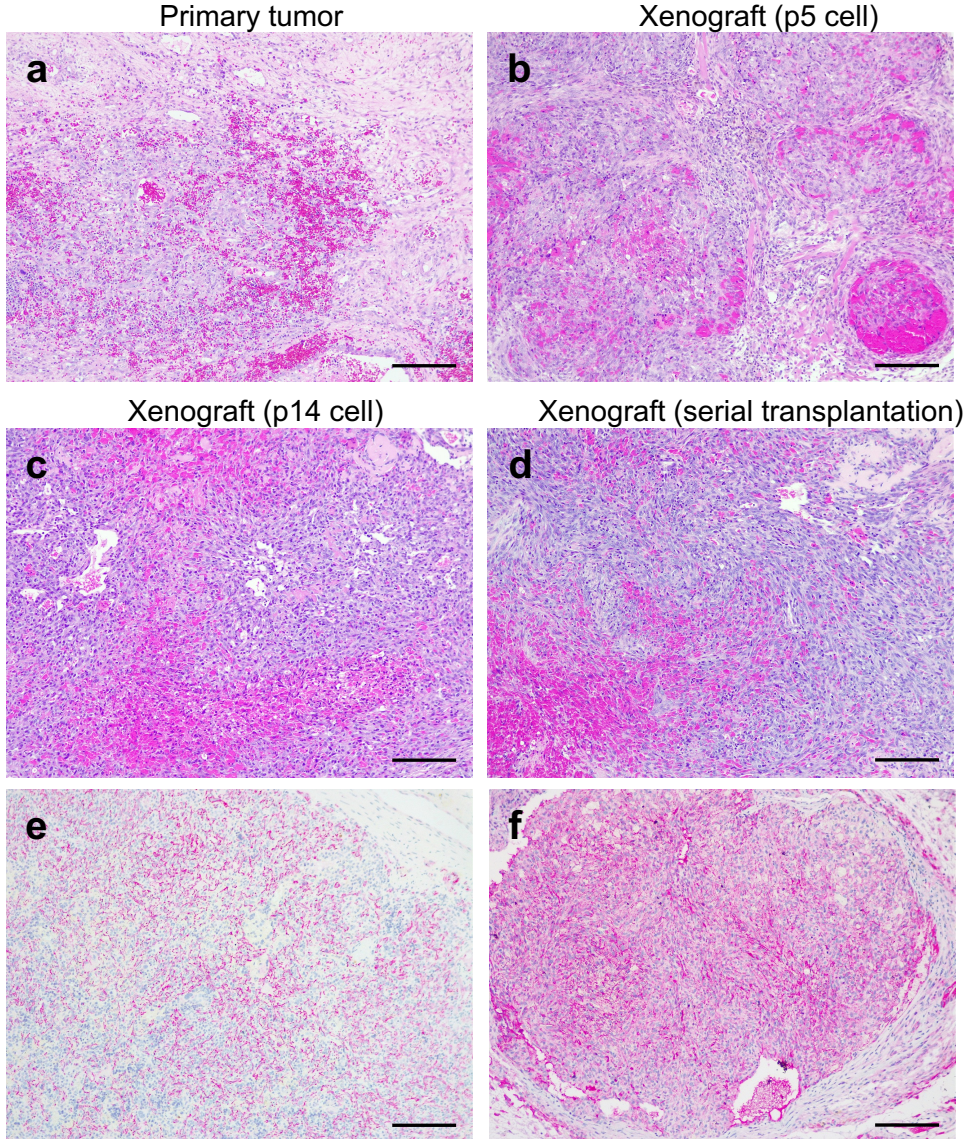
Primary tumor
Xenograft (p5 cell)
a
b
Xenograft (p14 cell)
Xenograft (serial transplantation)
c
d
e
f

Figure 1. Establishment of xenografts derived from canine hemangiosarcoma in immunodeficient mice. (**A**) Schematic illustration depicts process of tumor xenografts in beige-nude-xid (BNX) mice. (**B**) DHSA-1426 tumor cell line was established from a canine patient diagnosed with hemangiosarcoma (**a**). Cells from DHSA-1426 passages 5 (p5) and 14 (p14) formed tumors histologically classified as hemangiosarcoma (**b, c**). Cells cultured from xenograft-derived tumors developed histologically identical tumors after serial transplantation (**d**). Both the primary tumor (**e**) and the xenograft tumor (**f**) were positive for CD31 immunohistochemical staining. (a-d) Hematoxylin and eosin (H&E) stain. (e,f) Immunohistochemistry with an anti-CD31 antibody (alkaline phosphatase conjugates; counterstain = hematoxylin). Bar = 200 μm.

Figure 2

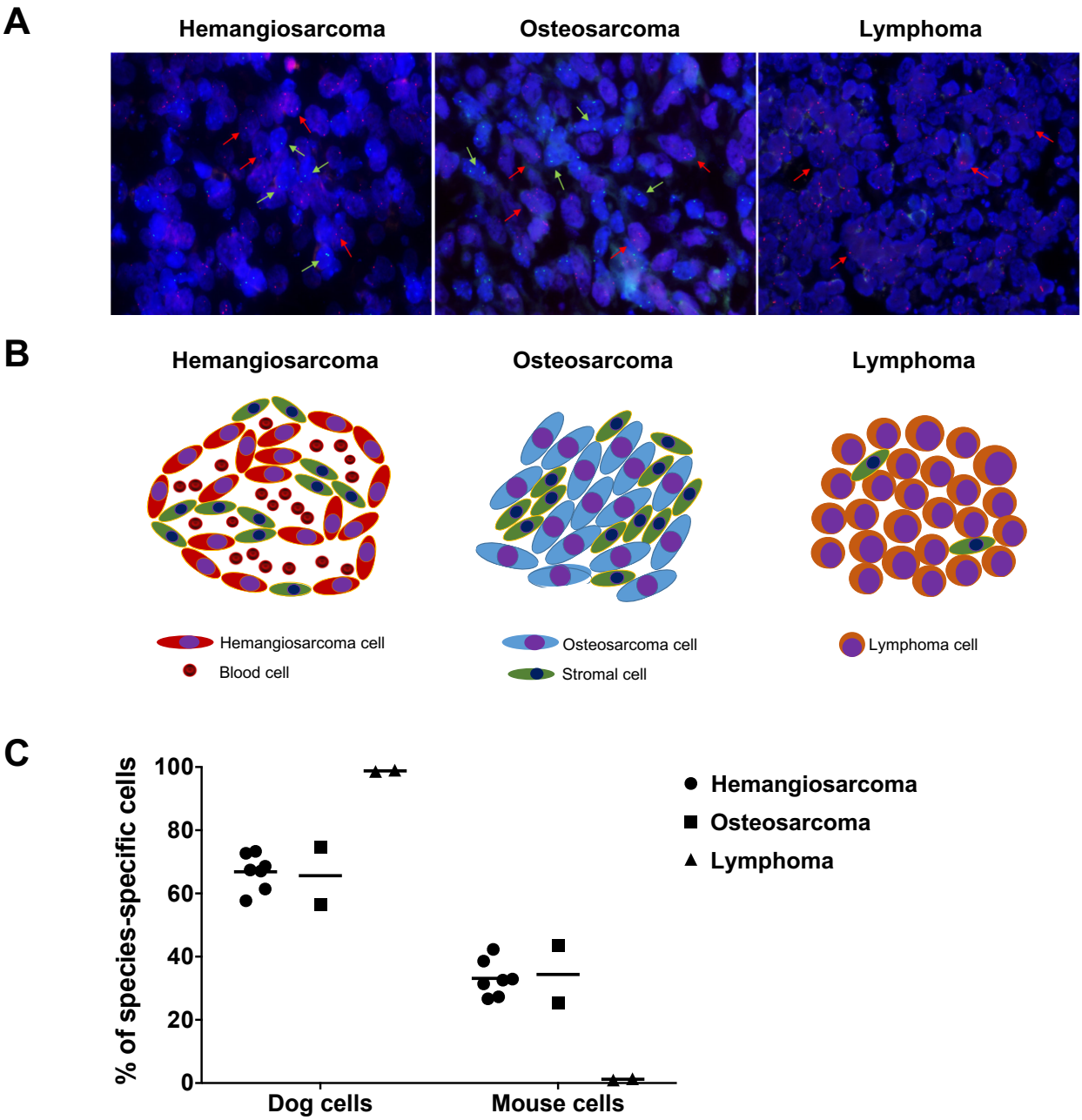
A
Hemangiosarcoma
Osteosarcoma
Lymphoma
B
Hemangiosarcoma
Osteosarcoma
Lymphoma
Hemangiosarcoma cell
Blood cell
Osteosarcoma cell
Stromal cell
Lymphoma cell
C
% of species-specific cells
100
80
60
40
20
0
Dog cells
Mouse cells
Hemangiosarcoma
Osteosarcoma
Lymphoma

Figure 2. Organization of tumor and stromal cells in mouse xenografts of canine hemangiosarcoma, osteosarcoma, and lymphoma. (**A**) Fluorescence *in situ* hybridization images using canine-specific (*CXCL8*, red) and mouse-specific (X chromosome, green) probes in a canine hemangiosarcoma xenograft, a canine osteosarcoma xenograft, and a canine lymphoma xenograft transplanted into receptive immunodeficient female mouse hosts. Red and green arrows point to representative xenograft canine tumor cells and mouse stromal cells, respectively, to aid in identification. (**B**) Schematic representation of A, illustrating the organization of hemangiosarcoma, osteosarcoma, and lymphoma xenografts. (**C**) Individual points on graph represent relative quantity of donor (dog) and host (mouse) cells in each tumor type. 10-12 fields of pictures at high magnification (400X) per slide were acquired. A total of approximately 1,000 cells in individual xenograft tumor was counted, and the percentages for each species-cells are presented.

Figure 3

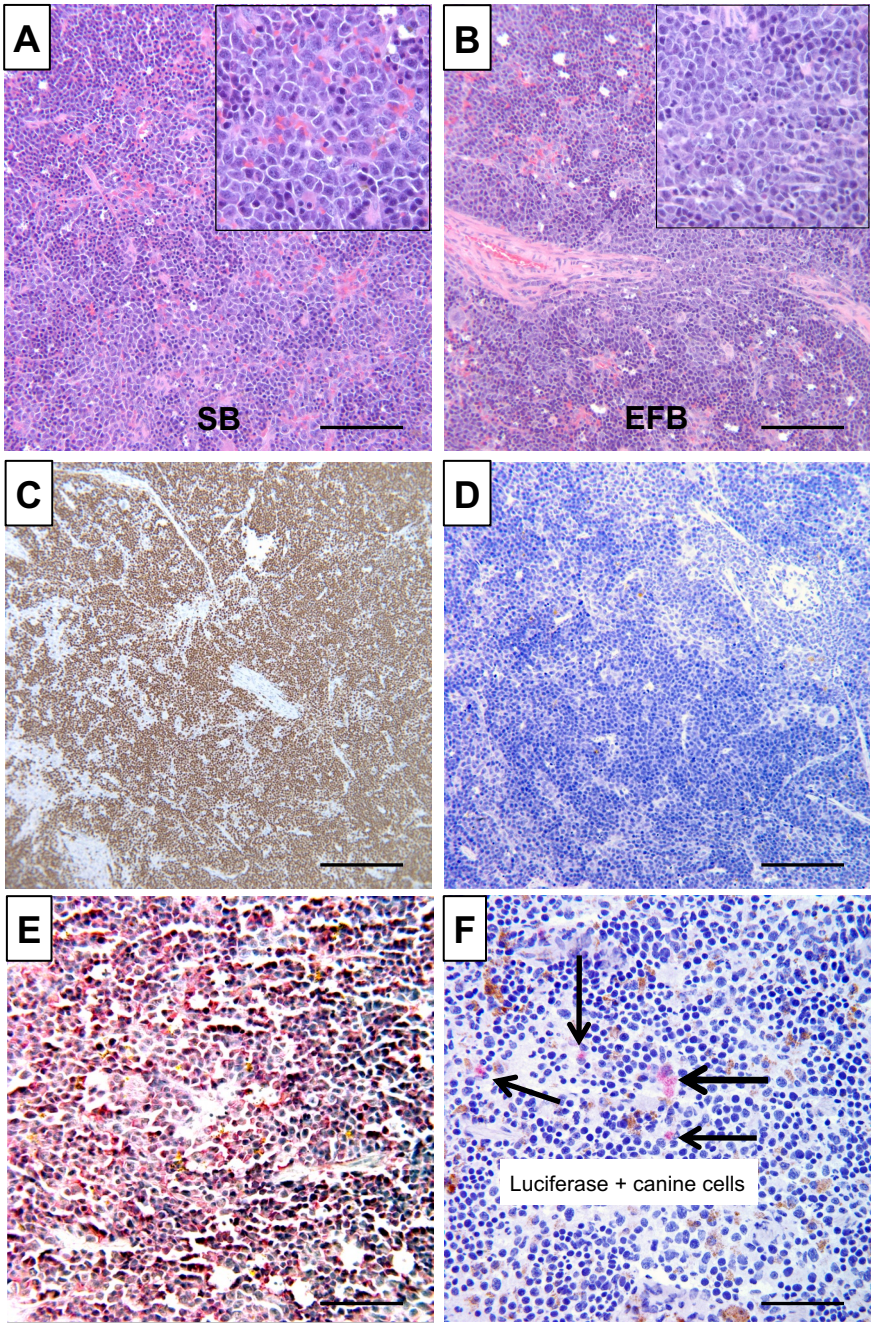

Figure 3. Hematopoietic expansion derived from adoptive transplantation of canine hemangiosarcoma in immunodeficient mice. (**A** and **B**) Xenotransplantation of canine hemangiosarcoma cell lines created exuberant myeloid hyperplasia in mouse spleens. Representative photomicrographs show histopathology by H&E staining of spleens from NSG mice transplanted with hemangiosarcoma cell lines SB (**A**) and EFB (**B**). (**C**) Immunoreactivity of anti-mouse Ki-67 (Tec-3) antibody shows strongly positive signal in proliferating cells in the spleen. (**D**) Immunostaining of anti-human (and canine cross- reactive) Ki-67 (MiB-1) antibody shows lack of positive staining among proliferating cells. (**E**) The proliferating cells are immunoreactive with anti-mouse Ter-119 antibody. (**F**) SB cells expressing Luciferase are detected in mouse spleen (arrows). Images shown in panels **C**, **D**, **E**, and **F** are from immunohistochemistry staining done in mice inoculated with SB cells modified to express GFP and firefly Luciferase. Horseradish peroxidase (for Ki-67 stains) and alkaline phosphatase (for Ter-119 and Luciferase) conjugates were used. Counterstain = hematoxylin. A-D: Bar = 200 µm; E-F: Bar = 50 µm.

Figure 4

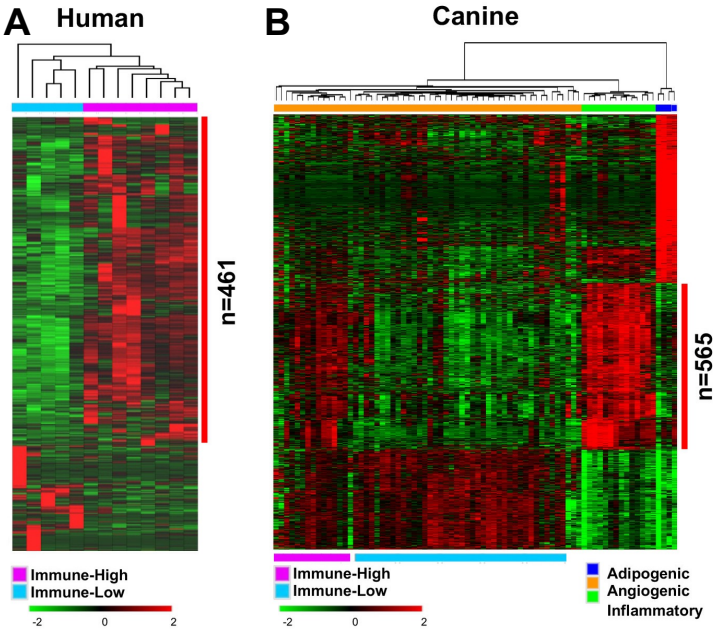

C

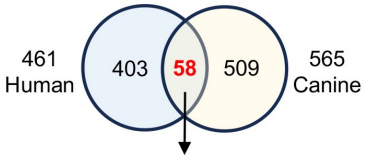

Pathways	P value	FDR P
B cell activation	3.3E-09	5.5E-07
T cell activation	2.2E-08	1.8E-06
Inflammation mediated by chemokine/cytokine signaling	1.5E-06	8.3E-05
Toll receptor signaling	1.0E-03	3.3E-02

Fisher's exact test

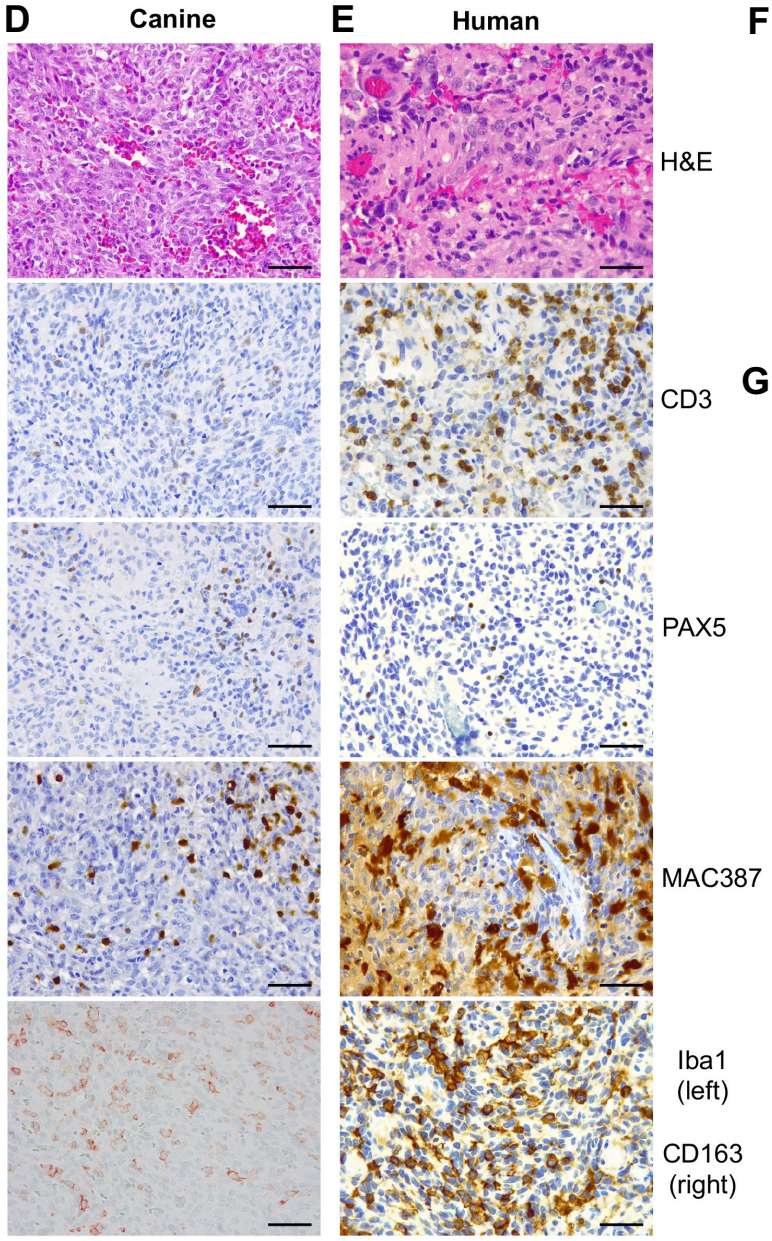

F

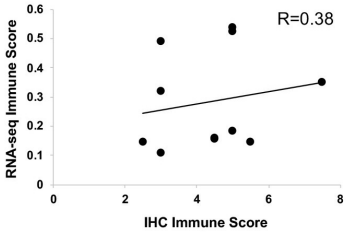

G

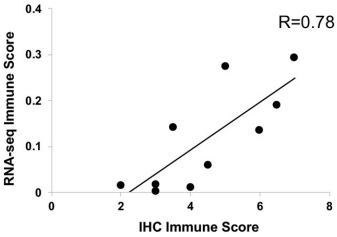

Figure 4. Immune cell infiltration and comparative immune signatures between canine hemangiosarcoma and human angiosarcoma. (**A**) 461 upregulated genes were identified in immune-high (N = 8) compared to immune-low (N = 5) groups in human angiosarcomas (FDR P value < 0.05). (**B**) 567 immune gene signatures were identified among three molecular subtypes of canine hemangiosarcomas (N = 76; FDR P value < 0.001; fold change > 3). The heatmaps show up-regulated (red) and down-regulated (green) genes by unsupervised hierarchical clustering (average linkage; mean-centered; $\log^2$ transformed). (**C**) Venn diagram shows 58 common genes associated with signaling pathways of immune cell functions between human and canine tumors. **(D** and **E)** Representative photomicrographs of H&E and immunohistochemical staining showing histological morphology and immune cell infiltration in canine hemangiosarcoma (**D**) and human angiosarcoma tissues (**E**) using anti-CD3, anti-PAX5, anti-MAC387, and anti-Iba1 (for canine) or anti-CD163 (for human) antibodies for detecting T cell, B cell, and macrophages. Horseradish peroxidase (counterstain = hematoxylin) or alkaline phosphate (for Iba1; counterstain = methylene blue). Bar = 50 um. (**F** and **G**) Scatter plots display correlation between transcriptional and immunohistochemical (IHC) immune score in canine hemangiosarcoma (**F**) and human angiosarcoma (**G**). Spearman's correlation coefficient (R) was calculated.

Figure 5

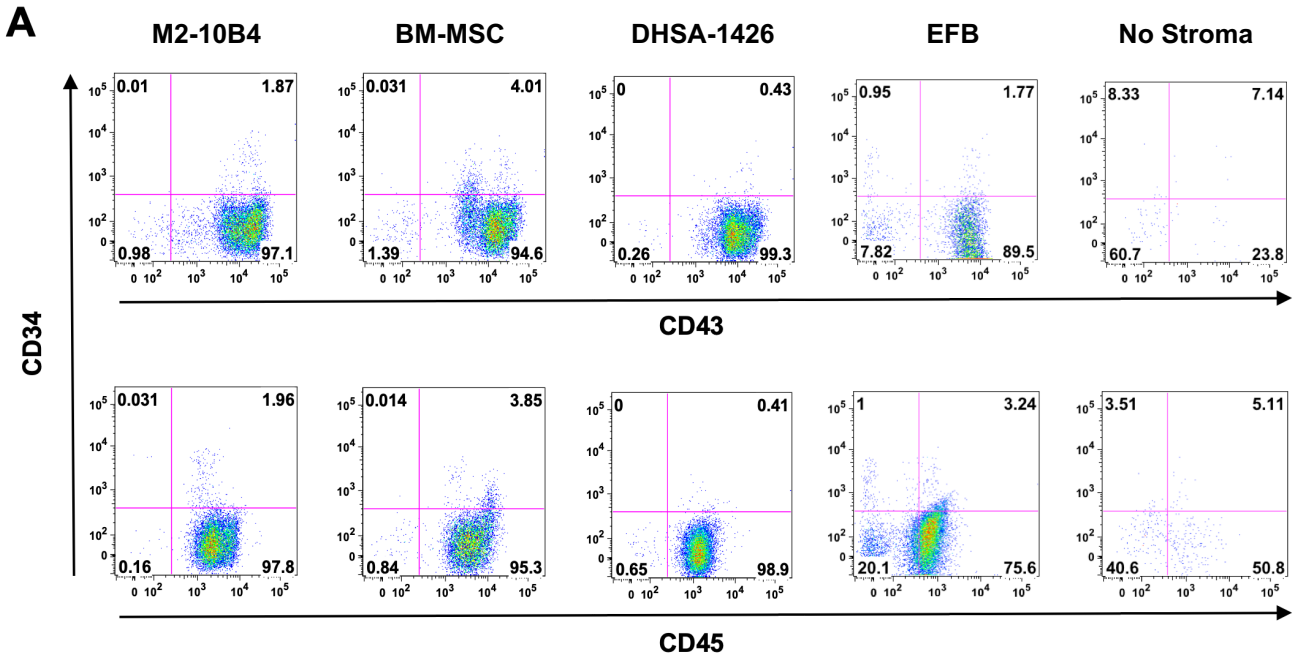
A
M2-10B4
BM-MSC
DHSA-1426
EFB
No Stroma
CD34
CD43
CD45
0.01
1.87
0.98
97.1
0.031
4.01
1.39
94.6
0
0.43
0.26
99.3
0.95
1.77
7.82
89.5
8.33
7.14
60.7
23.8
0.031
1.96
0.16
97.8
0.014
3.85
0.84
95.3
0
0.41
0.65
98.9
1
3.24
20.1
75.6
3.51
5.11
40.6
50.8

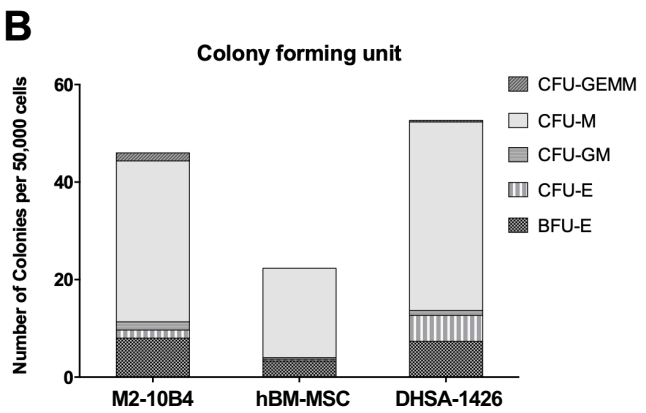
B
Colony forming unit
Number of Colonies per 50,000 cells
60
40
20
0
M2-10B4
hBM-MSC
DHSA-1426
CFU-GEMM
CFU-M
CFU-GM
CFU-E
BFU-E

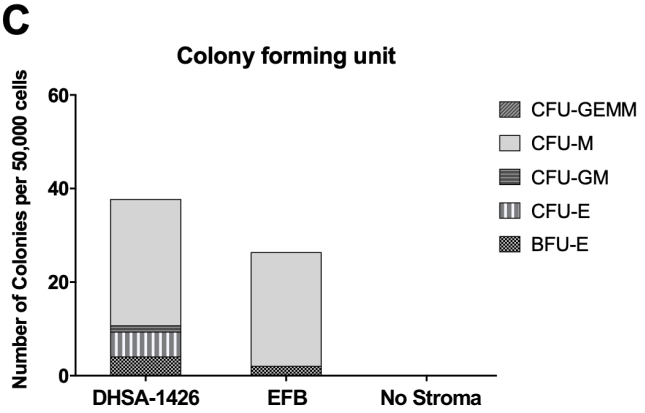
C
Colony forming unit
Number of Colonies per 50,000 cells
60
40
20
0
DHSA-1426
EFB
No Stroma
CFU-GEMM
CFU-M
CFU-GM
CFU-E
BFU-E

Figure 5. Canine hemangiosarcoma cells support expansion and differentiation of CD34+ human umbilical cord blood (hUCB) cells. (**A**) Flow cytometric data show populations of cells expressing CD43 and CD45 differentiated from CD34+ hUCB cells. CD34+ hUCB cells were pooled from two patients. M2-10B4, hBM-MSCs, and canine hemangiosarcoma cells (DHSA-1426 and EFB) were seeded on gelatin-coated 24-well plates at a density of $1x10^5$ cells/well. Gelatin-coated wells without stroma served as a negative control. Surface antigens of CD34, CD43, and CD45 were analyzed at week 5. (**B** and **C**) Bar graphs show number of different colonies formed by hUCB CD34+ cells co-cultured with feeder cells. Both DHSA-1426 and EFB canine hemangiosarcoma cell lines expanded hUCB CD34+ cells similar to the M2-10B4 and hBM-MSC positive control lines, while gelatin-coated wells alone failed to support expansion. Burst-forming unit-erythroid (BFU-E), CFU (colony-forming unit)-Erythroid (CFU-E), CFU-Granulocyte/Macrophage (CFU-GM), CFU-Macrophage (CFU-M), and CFU-Granulocyte/Erythroid/Macrophage/Megakaryocyte (CFU-GEMM) were determined for CFU assay.

Figure 6

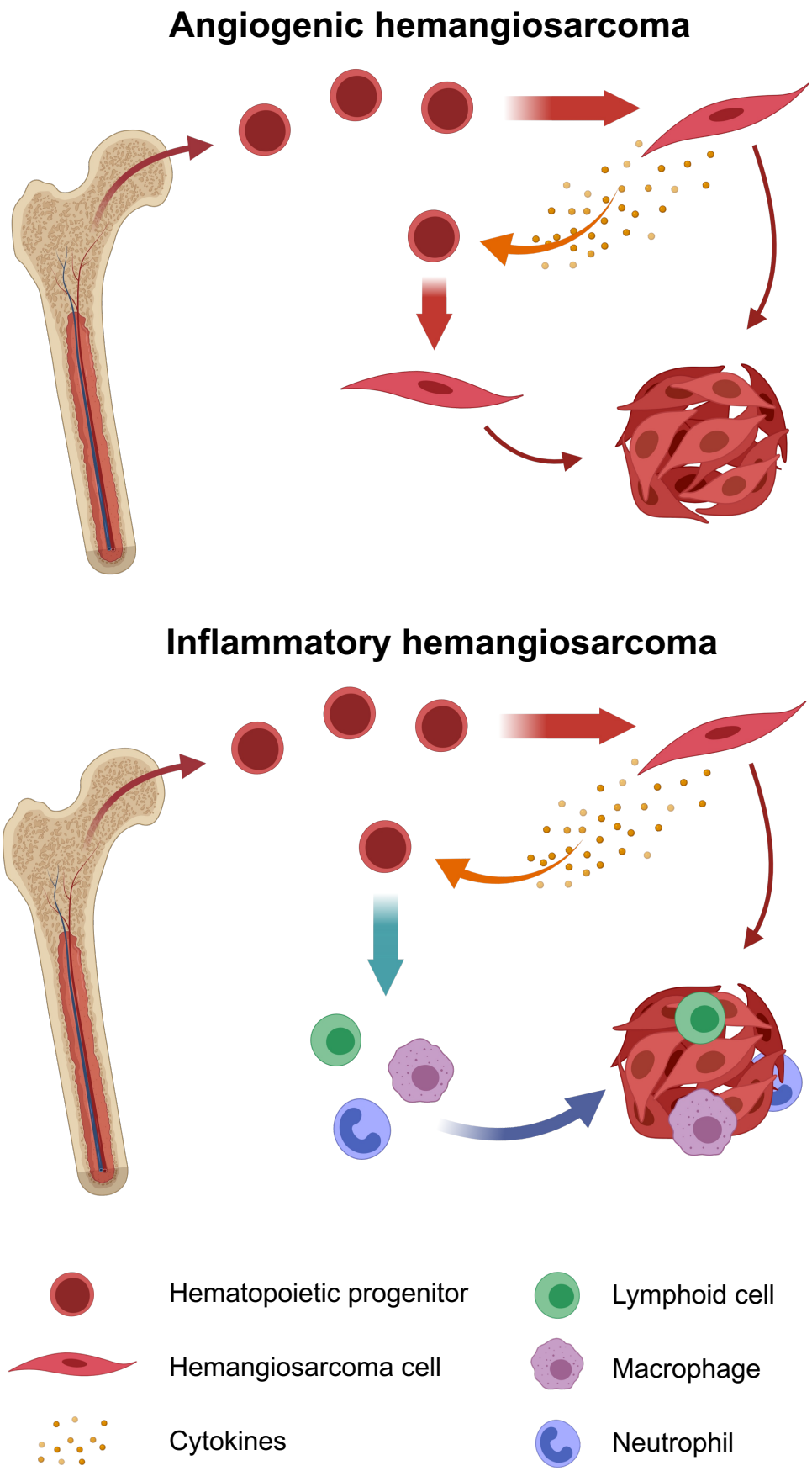
Angiogenic hemangiosarcoma
Inflammatory hemangiosarcoma
Hematopoietic progenitor
Hemangiosarcoma cell
Cytokines
Lymphoid cell
Macrophage
Neutrophil

Figure 6. Hypothetical models for establishment of distinct molecular phenotypes of canine hemangiosarcoma. Non-mutually exclusive models illustrate discreet cells of origin for distinct molecular subtypes of hemangiosarcoma. Hemangiosarcoma may progress from bone marrow nurse cells that create a niche for hematopoietic expansion and inflammation, to a transitional pro-angiogenic state and full progression to a pure angiogenic state, or to malignant transformation with an inflammatory phenotype.